

Supplementary Information

Liquid Crystalline Microspheres of Azobenzene Amphiphiles Formed by Thermally Induced pH Changes in Binary Water-Hydrolytic Ionic Liquid Media

Tejwant Singh Kang,^{a,c} Masa-aki Morikawa,^{a,b} Nobuo Kimizuka^{,a,b}*

^aDepartment of Chemistry and Biochemistry, Graduate School of Engineering, ^bCentre for Molecular Systems (CMS), Kyushu University, 744 Moto-oka, Nishi-ku, Fukuoka-819-0395, Japan. ^cDepartment of Chemistry, Guru Nanak Dev University, Amritsar-143005, Punjab, India.

Experimental Methods:

- 1. Amphiphile 1 and ionic liquids:** Azobenzene amphiphile **1** (Scheme 1, main text) was synthesized according to the procedure described in the literature.¹ Amphiphile **1** was recrystallized twice from ethanol which appeared in the form of orange plates. The synthesized amphiphile **1** was analyzed through ¹H NMR and FTIR spectroscopies. High purity ILs were procured from Kanto Chemical Co., Inc (1-ethyl-3-methylimidazolium tetrafluoroborate, [C₂mim][BF₄]; 1-ethyl-3-methylimidazolium ethylsulfate, [C₂mim][C₂OSO₃]) and Io-li-tec (*N*-methyl pyridinium tetrafluoroborate, [C₂Py][BF₄]; *N*-ethyl-*N*-propyl pipyridinium tetrafluoroborate, [C₁C₃Py][BF₄]; and *N*-ethyl-*N*-methyl pyrrolidinium tetrafluoroborate, [C₂C₁Pyrr][BF₄]).
 - 2. Preparation of dispersions:** Dispersions of amphiphile **1** in IL-water binary solvent mixtures (2, 10, 30, 60 and 90 vol% IL) of various ILs were prepared by the following procedure. First, methanol solutions of amphiphile **1** were prepared. After removal of methanol via N₂ purging, the required amount of freshly prepared IL-water binary mixtures were added to make final required concentrations of amphiphile **1**. Although amphiphile **1** is readily dispersed in binary IL-water solutions by just shaking, all the dispersions were sonicated for about 5 minutes to ensure the macroscopic homogeneity (Yamato-1500 BRANSON water sonicator). For all the measurements, the concentration of **1** was kept 500 μM, which is above its critical aggregation concentration (*cac*), if not stated otherwise.
- ### 3. Methods:
- 3.1. Dynamic light scattering measurements:** Dynamic light scattering (DLS) measurements were performed on Zeta-Sizer, nano-series (nano-ZS) Malvern Instruments equipped with an in-build temperature controller (accuracy, ± 0.1 K) using a small volume quartz cuvette. An average of 10 measurements for each sample has been entertained as the data. Prior to each measurement, the samples were stabilized for 5 minutes at respective temperatures for thermal equilibration. DLS measurements were made a scattering angle of 173°. DLS count rate measurements were conducted for newly prepared dispersions.
 - 3.2. Optical microscopy measurements:** Optical microscopy (dark field, a bright field and polarized) was performed using a Nikon optical microscope (Nikon Eclipse 80i). For the measurement, a drop of the sample was taken on a freshly cleaned glass slide followed by covering it with coverslip. In general, measurements have been made at 20X or 100X magnification.
 - 3.3. Transmission electron microscopy measurements:** Transmission electron microscopy (TEM) was performed on a JEOL JEM-2010 electron microscope at a working voltage of 120 kV. Samples were prepared by putting a drop of various dispersions of amphiphile **1** (500 μM) on the carbon-coated copper grid followed by blotting off the residual liquid

immediately to decrease the change in pH of the dispersion with time. The samples were post-stained with uranyl acetate and dried at room temperature.

3.4. Scanning electron microscopy: Scanning electron microscopy was performed on a Hitachi S-5000 scanning electron microscope. For SEM measurements, samples were dropped on carbon-coated copper grids used for TEM measurements, and residual liquid was blotted off. The samples were dried in vacuum at room temperature. Before measurement, the samples were coated with platinum in vacuo.

3.5. UV-vis absorption measurements: UV-vis absorption spectra were measured using a JASCO 660 spectrophotometer equipped with an in-built temperature controller (accuracy, ± 0.1 K) using quartz cuvette of path length 1 mm. All the samples were equilibrated for about 10 minutes before each measurement.

3.6. pH measurements: pH measurements were made using a HORIBA compact pH meter, B-212. Before measurements, the pH meter was calibrated with buffer solutions of pH 4.0 and 7.0 at room temperature.

3.7. ^1H NMR measurements: ^1H NMR spectrum of amphiphile **1** was measured using a JEOL 400 NMR spectrometer in CD_3OD .

3.8. FTIR measurements: FT-IR spectra were recorded on a Varian 660 IR spectrometer using the KBr pellet method in the range of $600\text{--}4000\text{ cm}^{-1}$.

3.9. Powder-XRD measurements: Wide angle X-ray scattering measurements were performed using Rigaku Xpert Pro X-ray diffractometer having $\text{Cu K}\alpha$ radiation (1.541\AA) operated at 40 kV of voltage and at a current of 30 mA. The scan was performed in the 2θ range from $20\text{--}85^\circ$ with a step size of 0.02° .

4. Annexure SI: Nematic liquid crystalline microspheres (LCMs) have been prepared by the following steps:

- (1) First, a methanol solution of amphiphile **1** was prepared at a concentration of 3.0 mM and taken into a Teflon coated glass vial in an appropriate amount followed by purging of N_2 to remove methanol.
- (2) Very freshly prepared (within a minute) IL-water binary mixture at varying compositions (2, 10, 30, 60 and 90 vol%) was put into the vial having amphiphile **1** in an appropriate amount to make the final concentration of amphiphile **1** as $500\text{ }\mu\text{M}$ (*above critical aggregation concentration in all the cases*). At this stage, the pH of the solution was checked as the investigated ILs with BF_4 anion are hydrolytic. This lowers the pH of the solution.²
- (3) The solution was taken into a small volume quartz cuvette (path length 1 mm) for UV-vis measurements immediately (within 5 minutes of preparation of dispersion) after its preparation at room temperature. The presence of nano-aggregates in binary IL-water systems was observed by dark-field optical microscopy and TEM. The amphiphile **1** was not

protonated at this stage. The self-assembly of amphiphile **1** in non-hydrolytic IL, [C₂mim][C₂OSO₃]-water system has been established by our research group.³

- (4) The solution was heated up to 95 °C for 15 minutes in the closed cuvette to nullify the water loss and cooled down to room temperature while shaking, and the specimens were characterized as described in step 3. The amphiphile **1** present in the binary water-IL solution at this stage becomes protonated as indicated by the change in UV-vis absorption spectra and change in color of the dispersion from yellowish to pinkish in color.⁴
- (5) The process of heating and cooling was repeated at least 3 times and the solution was kept at room temperature for another 30 minutes. After this period, one could observe slight turbidity in the cuvette, indicating the formation of large aggregates. The aggregate structures in these IL-water systems were monitored by dark field and bright field optical microscopes. The LCMs prepared at this stage were investigated by TEM, SEM, and optical microscopy.
- (6) At every stage, DLS measurements were conducted to characterize the size of aggregates.
- (7) TEM and SEM measurements were made only for the representative IL-water system ([C₂mim][BF₄]-water with 10 vol% of IL).
- (8) The formation of LCMs was observed up to the IL content of 30 vol% in the IL-water mixtures.

References

1. Kunitake, T.; Okahata, Y.; Shimomura, M.; Yasunami, S.; Takarabe, K. Formation of Stable Bilayer Assemblies in Water from Single-Chain Amphiphiles. The relationship between the Amphiphile Structure and the Aggregate Morphology. *J. Am. Chem. Soc.*, **1981**, *103*, 5401-5413.
2. Freire, M. G.; Neves, C. M. S. S.; Marrucho, I. M.; Coutinho, J. A. P.; Fernandes, A. M. Hydrolysis of Tetrafluoroborate and Hexafluorophosphate Counter Ions in Imidazolium-Based Ionic Liquids. *J. Phys. Chem. A*. **2010**, *114*, 3744-3749.
3. Kang, T. S.; Ishiba, K.; Morikawa, M.-a.; Kimizuka, N. Self-Assembly of Azobenzene Bilayer Membranes in Binary Ionic Liquid–Water Nanostructured Media. *Langmuir*, **2014**, *30*, 2376-2384.
4. Oakes, J.; Gratton, P. Kinetic Investigations of the Oxidation of Methyl Orange and Substituted Arylazonaphthol Dyes by Peracids in Aqueous Solution. *J. Chem. Soc., Perkin Trans.2*, **1998**, 2563–2568.

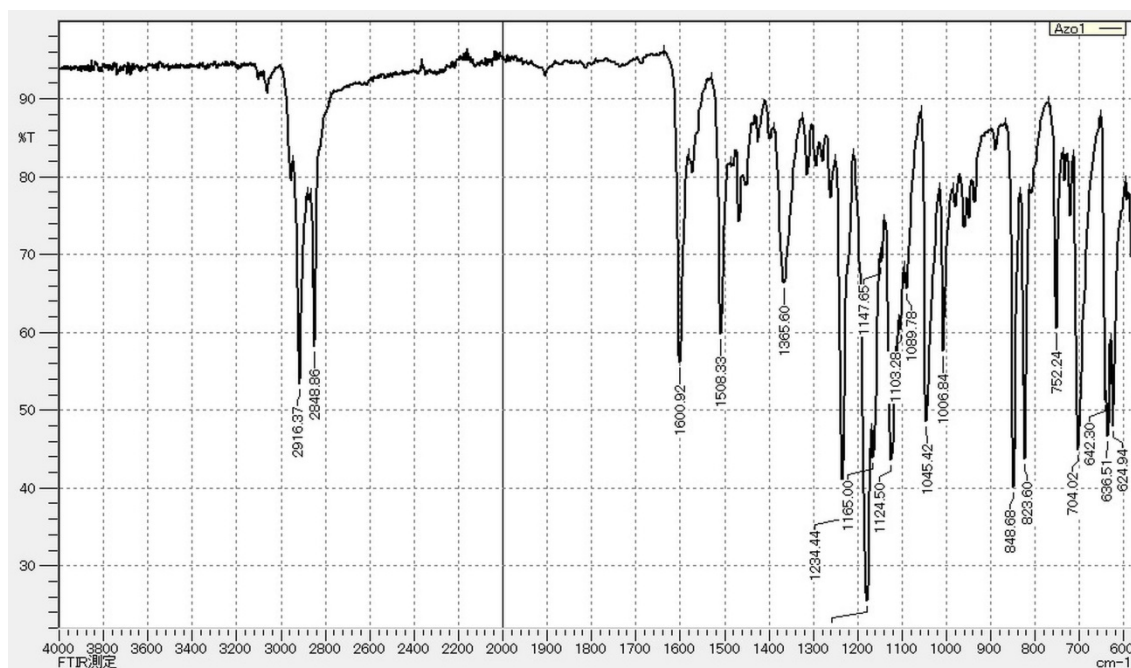
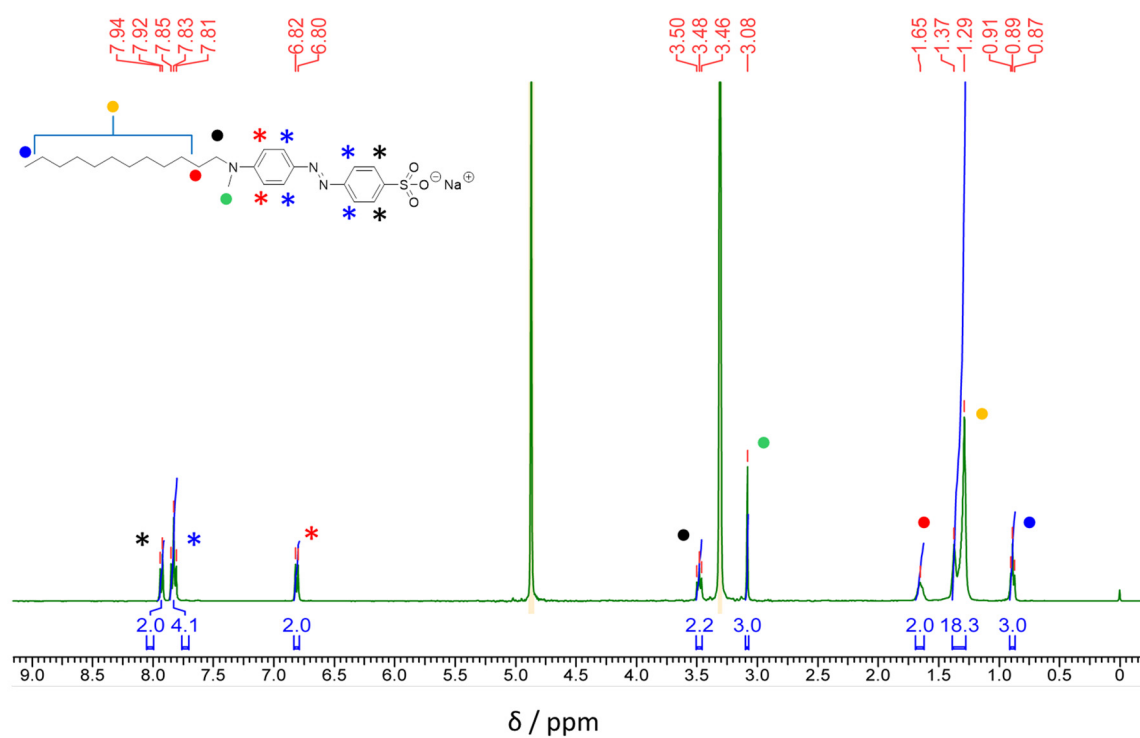


Fig. S1: (A) ¹H NMR spectrum in CD₃OD and (B) FTIR spectrum of amphiphile 1.

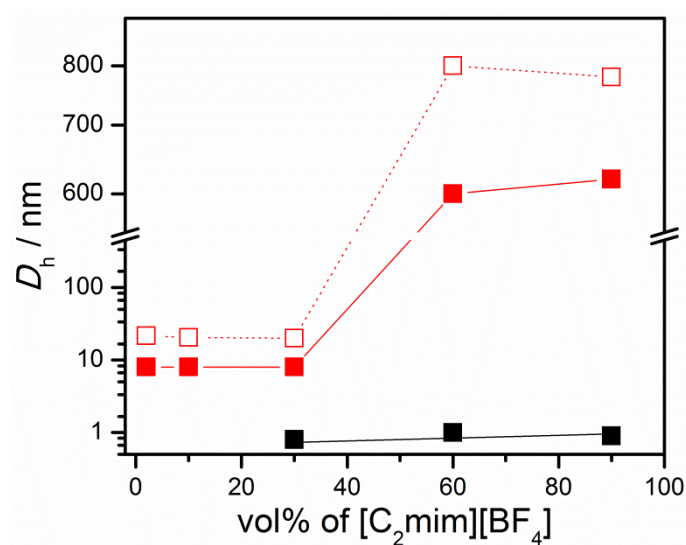


Fig. S2. Variation of hydrodynamic diameter (D_h) in binary water–[C₂mim][BF₄] mixtures in the absence (filled square in black) and presence of amphiphile **1** (filled square in red, 500 μ M of **1**, above *cac*) as a function of the IL content in binary water–IL mixtures at 25 °C. The open square in red, heat-cooled samples; the specimens were heated once to 95 °C and then cooled down to 25 °C.

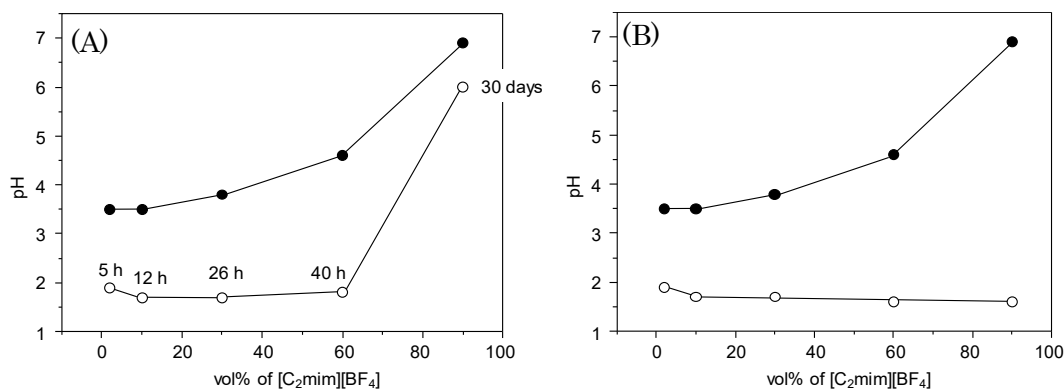


Fig. S3. Variation in pH of water–[C₂mim][BF₄] binary mixtures having amphiphile **1** (500 μ M) as a function of the content of IL in the binary mixture. (A) just prepared dispersion at 25 °C (Filled circle), and dispersions after given period required to achieve almost stable pH (open circle). (B) Variation of pH under similar conditions of the content of amphiphile **1** (500 μ M) and IL for just prepared (Filled circle, same data as in (A)) and dispersions after the heat-cooling treatment (open circle) at 25 °C. Heat-cooling treatment refers to the heating of the mixture to 95 °C for 15 minutes, and then cooling down to room temperature.

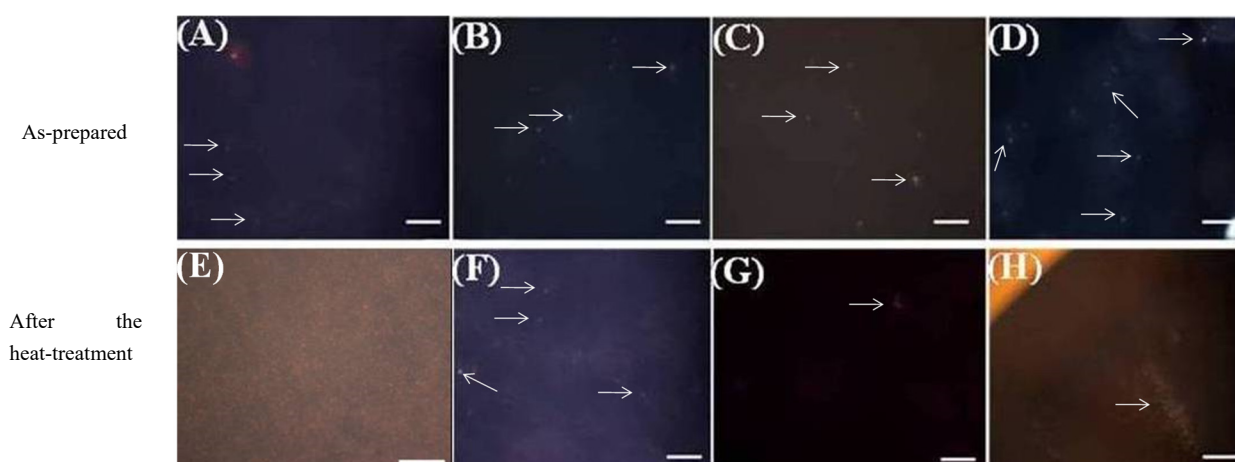


Fig. S4. Darkfield optical microscopic (DFOM) images of amphiphile **1** (500 μM , above *cac*) dispersed in water- $[\text{C}_2\text{mim}][\text{BF}_4]$ mixtures. (A) 2 vol%, (B) 10 vol%, (C) 30 vol% and (D) 60 vol% of IL at 25 $^\circ\text{C}$ (as-prepared dispersions). The corresponding DFOM images of (E), (F), (G) and (H) are taken after a heating-cooling cycle at 25 $^\circ\text{C}$ (after hydrolysis of $[\text{BF}_4]^-$). Clear images were not obtainable in an aqueous-IL mixture having 90 vol% of IL due to very high viscosity. The scale bars represent 5 μm .

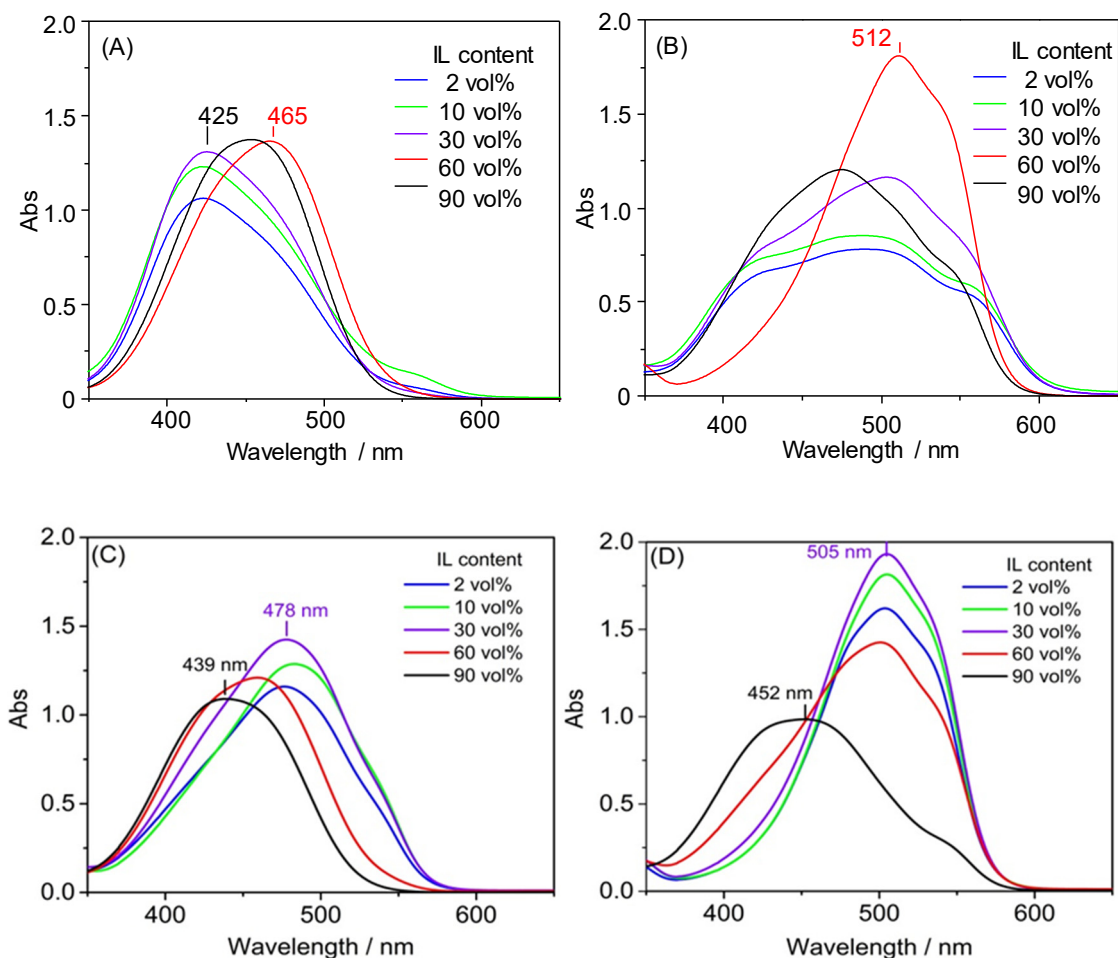


Fig. S5. UV-vis absorption spectra of (A) as prepared dispersions of amphiphile **1** and (B) after one heat-cooling cycle in different water–[C₂mim][BF₄] binary mixtures at 25 °C. [1] = 500 μM. (C) and (D) represents the UV-vis absorption spectra of Methyl orange (MO) under the same conditions as (A) and (B), respectively. [MO] = 500 μM. (C) as prepared dispersions and (D) after one heat-cooling cycle in different water–[C₂mim][BF₄] binary mixtures at 25 °C. Heat-cooling cycle refers to the heating of the mixture to 95 °C for 15 minutes, and then cooled down to room temperature.

The blue-shifted spectra were observed for dispersions with the IL content of 2-30 vol% (Fig. S5A). Meanwhile, at higher IL content (60 vol%), the as-prepared dispersions showed a λ_{max} at 465 nm (red curve in Fig. S5A). As the freshly prepared binary mixture showed the moderate pH (ca. 4.5) at this volume fraction (60 vol% [C₂mim][BF₄], Fig. S3), the azobenzene moiety is not protonated. The observed λ_{max} at 465 nm is close to that observed for monomerically dissolved MO in water–[C₂mim][C₂OSO₃] mixtures at room temperature and those of the liquid crystalline bilayers of **1** at temperatures above 55 °C.^{6b} We assign the 465 nm-species of **1** to

swollen liquid crystalline bilayer aggregates on the basis of DLS and DFOM results (Fig. S2 and Fig. S4D). It is reasonable that the intermolecular interactions among azobenzene amphiphiles are weakened at the higher IL content (60 vol%) even at room temperature. After the heat treatment, a single salient band with λ_{max} at 512 nm was observed for the binary mixture (IL: 60 vol%, Fig. S5(B)). It marks almost complete protonation of **1**. As liquid crystalline bilayers as-dispersed in the binary mixture with high IL content (IL: 60 vol%) showed weak intermolecular interactions as described above (Fig. S5A), it is reasonable that the heat-treatment promoted the protonation of **1**.

Figure S5(C, D) show spectra observed for methyl orange (MO) as a reference. MO does not form aggregates in water-IL binary mixtures. The absorption peak λ_{max} at ≈ 478 nm in aqueous [C₂mim][BF₄] (IL content, 2-30 vol%) is consistent with its monomeric form (Fig. S5C). At higher content of IL (IL: 90 vol%), MO displays spectral blue shift, which is a typical solvent polarity effect. A similar absorbance feature was observed for **1** under similar conditions, indicating the formation of loose aggregates in the high-IL content media as we discussed in the manuscript. After the heat-treatment (Fig. S5(D)), MO showed a single salient band with λ_{max} at 505 nm in the binary mixture (IL: 2-60 vol%). It marks complete protonation of MO. The complete protonation of monomeric MO at lower content of IL (IL: 2-30 vol%, Fig. S5(D)) is in contrast to that observed for **1** in the self-assemblies.

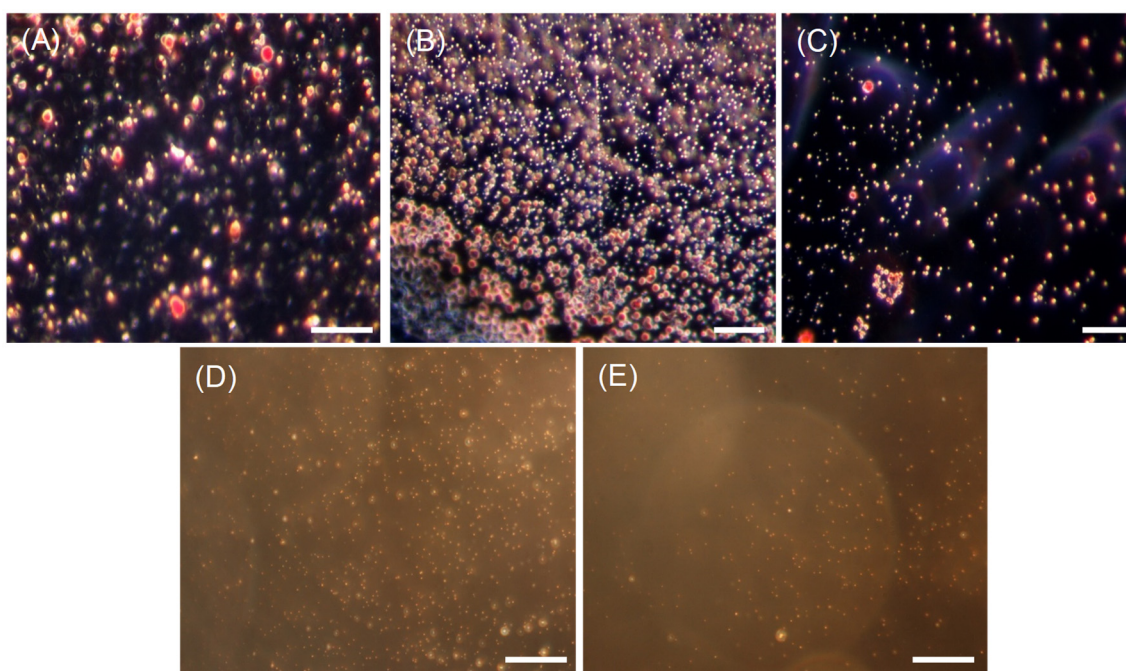


Fig. S6. Dark field optical microscopic images of the heat-cooled dispersions of **1** in binary water–IL mixtures at different vol% of [C₂mim][BF₄]; (A) 2 vol%, (B) 10 vol%, (C) 30 vol%, (D) 60 vol% and (E) 90 vol%. [**1**] = 500 μM, scale bar is 10 μm.

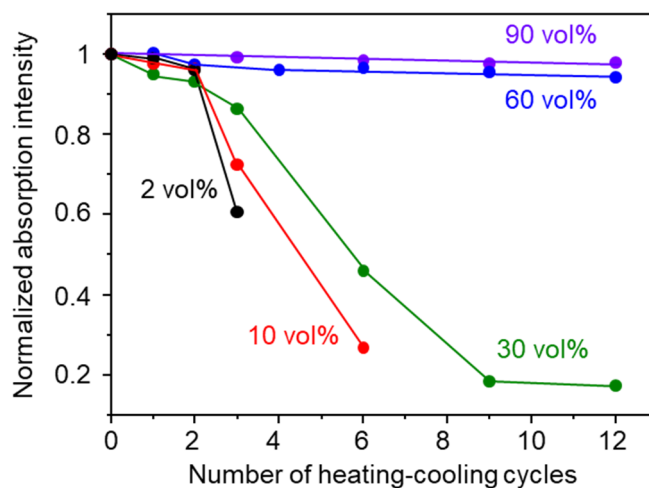


Fig. S7. Changes in (A) UV-vis absorption intensity at peak maximum of amphiphile **1** dispersed in various water–[C₂mim][BF₄] binary mixtures as a function of the number of heating-cooling cycles. [**1**] = 500 μM at 25 °C.

Upon repeated heating-cooling cycles, the size of LCMs increases in binary water–[C₂mim][BF₄] mixtures (IL: 2–30 vol%) (Fig. S8). Eventually, LCMs precipitate from the binary mixtures. This process is reflected in the decrease in the absorption intensity (Fig. S7).

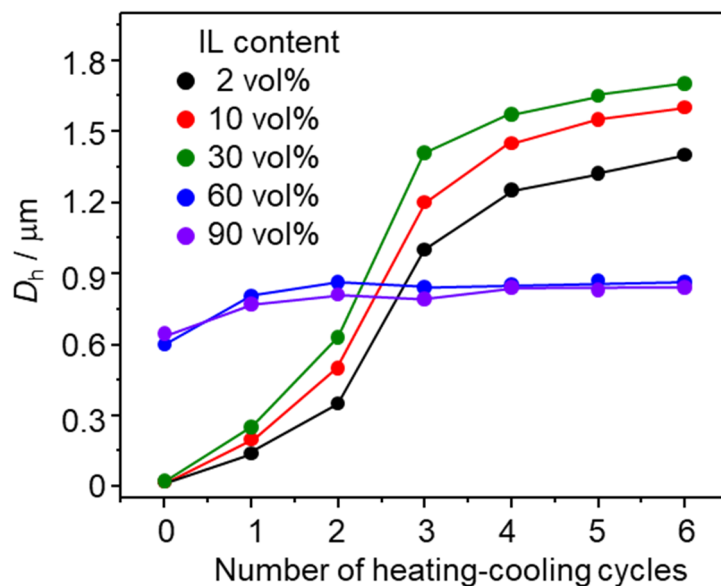


Fig. S8. Changes in hydrodynamic diameter (D_h) of amphiphile **1** dispersed in various water–[C₂mim][BF₄] binary mixtures as a function of the number of heating-cooling cycles. [**1**] = 500 μ M at 25 °C.

Amphiphile **1** self-assembles in the form of large swollen liquid crystalline bilayer aggregates at higher IL content and hence displays large D_h even at room temperature. Amphiphiles **1** in the water–[C₂mim][BF₄] binary mixture with high IL contents (IL: 60 and 90 vol%) are less protonated (Fig. S5B), and accordingly they are not affected by the heat-treatment as shown in Fig. S8. Under these conditions (IL: 60 and 90 vol%), LCMs are not formed. This is consistent with the unchanged absorption intensity of **1** in the water–[C₂mim][BF₄] binary mixtures (IL: 60 and 90 vol%, Fig. S7).

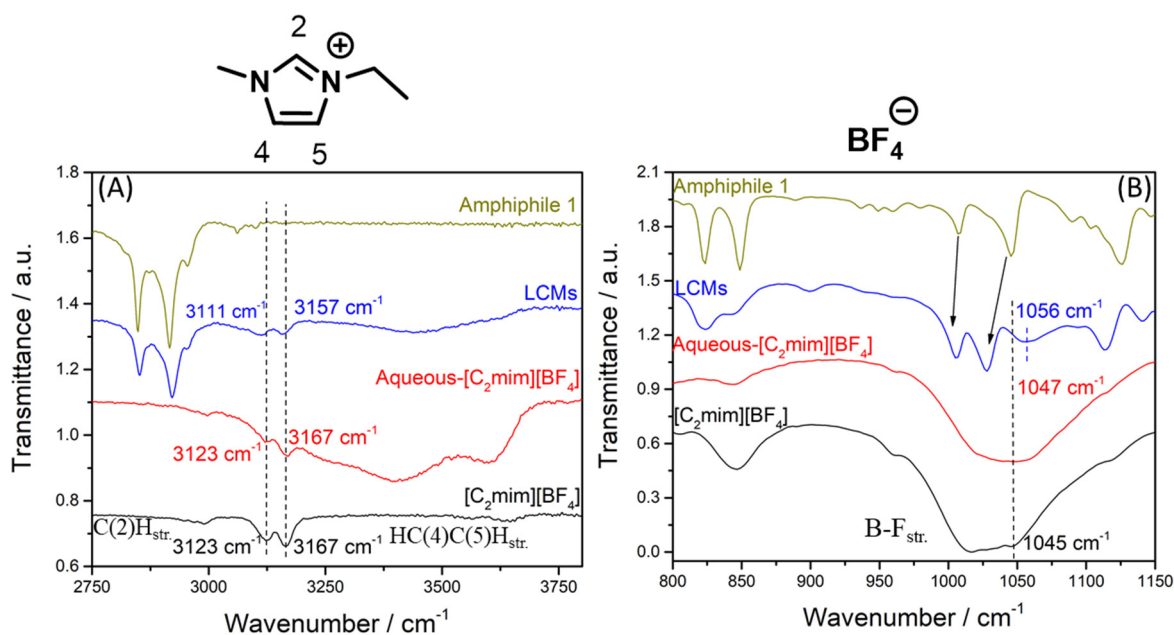


Fig. S9. FTIR spectra showing (A) C(2)H stretching and HC(4)C(5)H stretching of [C₂mim]⁺ and (B) B-F stretching of [BF₄]⁻ in neat IL, IL-water binary mixture, and LCMs in comparison to amphiphiles **1**.

The complexation of both [C₂mim]⁺ and [BF₄]⁻ with **1** in LCMs is supported by FTIR-spectroscopy. The CH stretching vibrations of imidazolium cation, C(2)H and HC(4)C(5)H, appeared at 3123 and 3167 cm⁻¹, respectively in neat IL. This IR spectrum is similar to that reported for [C₄mim][BF₄] (Singh et al., *Vibrational Spectroscopy* 55, 119–125, 2011). These frequencies don't shift in the binary aqueous-IL mixture as also reported in the literature (Singh et al., *Vibrational Spectroscopy* 55, 119–125, 2011). However, the stretching for C(2)H and HC(4)C(5)H appeared at 3110 and 3158 cm⁻¹, respectively in LCMs, indicating their involvement in the LCM phase.

Meanwhile, the B-F stretching of [BF₄]⁻ in IL appears as an intense broad band with shoulders around at 1017, 1033, and 1045 cm⁻¹, which is also in line with the reported values (Holomb et al., *J. Raman Spectrosc.* 39, 793–805, 2008).

Interestingly, we observed the shift of 1045 cm⁻¹–band in LCMs as compared to those in neat IL and aqueous-[C₂mim][BF₄] mixture (IL: 10 vol%). This shows the involvement of BF₄⁻ anions in LCMs.

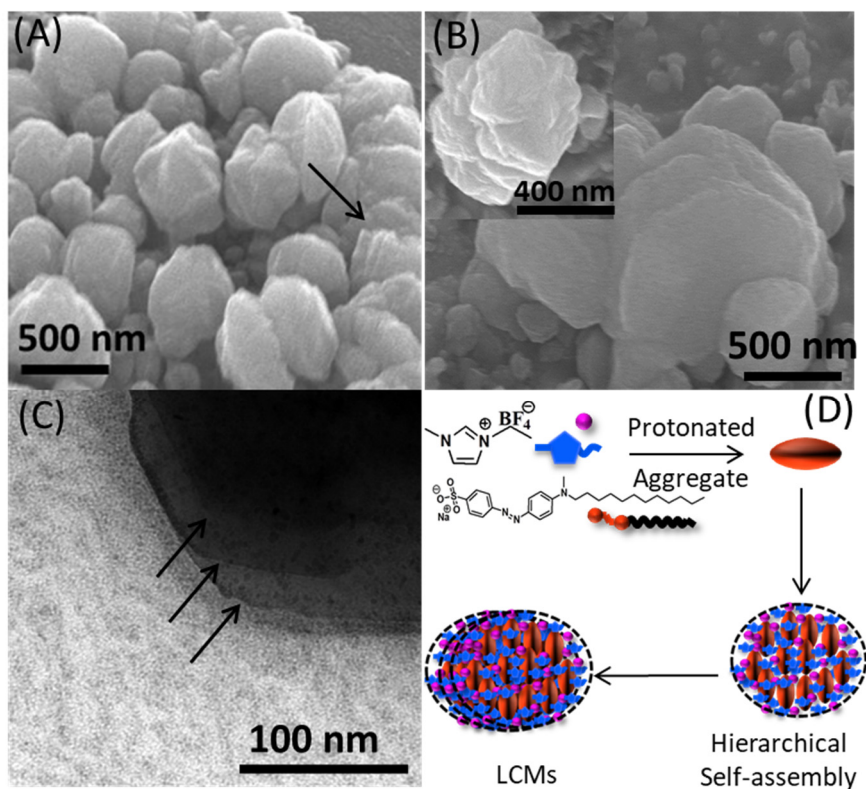


Fig. S10. (A) A scanning electron microscopic image of **1** dispersed in water–[C₂mim][BF₄] (IL content; 10 vol%) binary mixture after three heating-cooling procedures. The sample was vacuum coated with platinum. (B) shows the presence of a layered structure of LCMs, which is also evidenced by (C) TEM images (post-stained with uranyl acetate). Arrows in (C) indicates the presence of a layered structure of LCMs. (D) shows a schematic representation of the formation of LCMs.

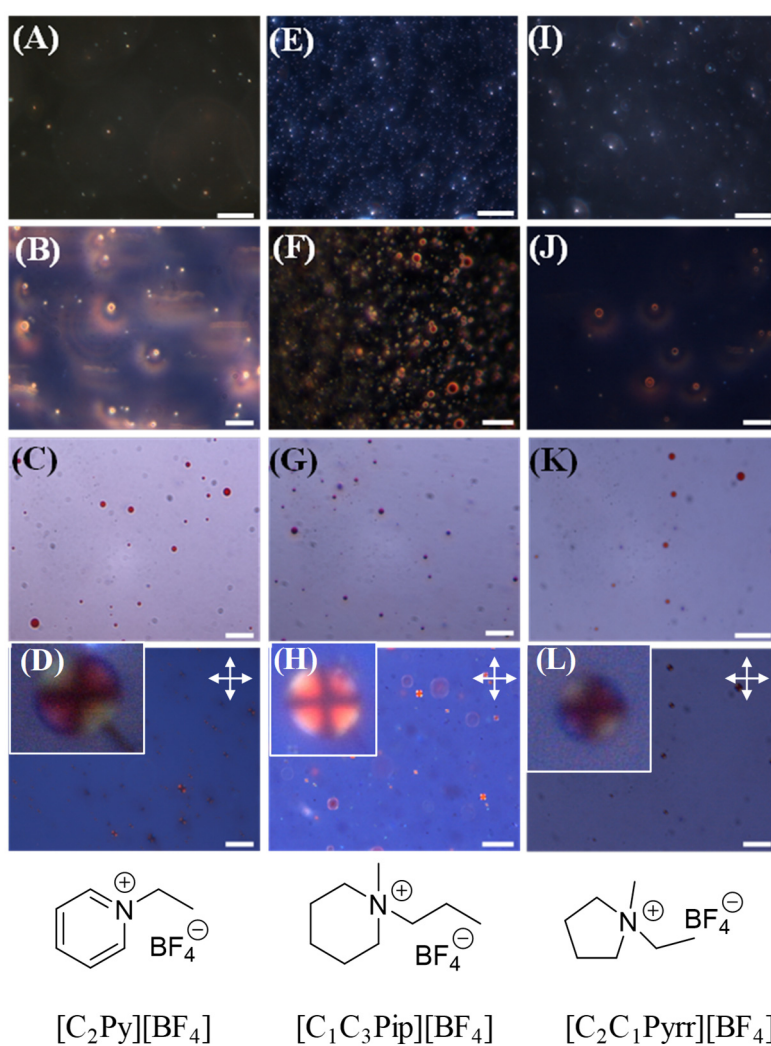


Fig. S11. Optical microscopic images of amphiphile **1** (500 μM) dispersed in different water-IL (IL; 10 vol %) binary mixtures. (A-D) [C₂Py][BF₄]; (E-H) [C₁C₃Pip][BF₄]; (I-L) [C₂C₁Pyr][BF₄]. (A), (E), and (I) are dark field optical microscopy (DFOM) images of as-prepared dispersions. (B), (F), and (J) are DFOM images after three heating-cooling cycles. (C), (G), and (K) are bright field images, and (D), (H), and (L) are polarized microscopy images after three heating-cooling cycles. Inset in (D), (H), (L) shows the enlarged view of one of the LCMs. Scale bar is 5 μm .

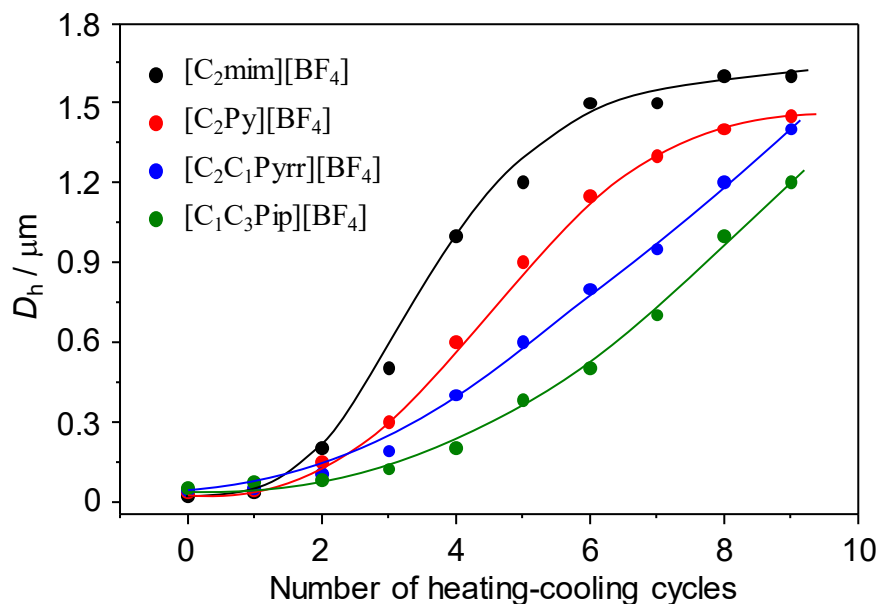


Fig. S12. Variation in D_h of aggregates formed in various binary water-ILs (ILs; 10 vol%) mixtures as a function of the number of heating-cooling cycles. The zero cycle refers to as prepared dispersions.

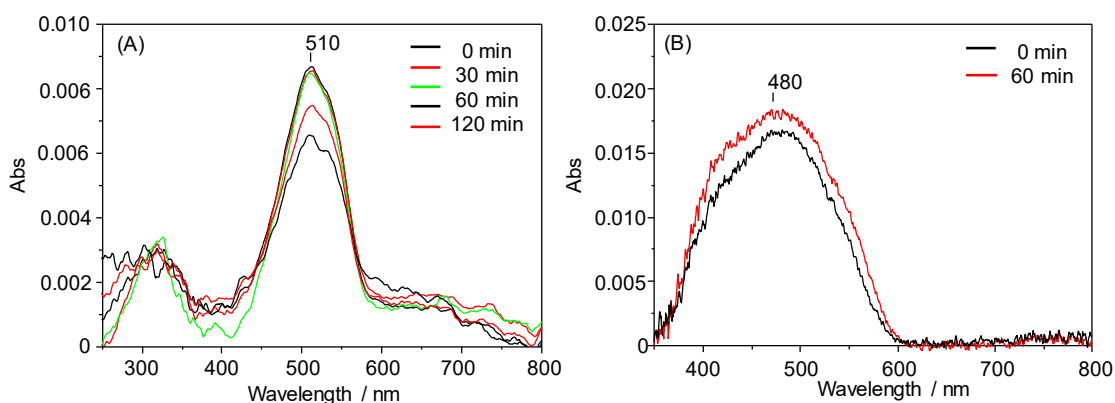


Fig. S13. UV-vis absorption spectra of amphiphile **1** (20 μM , above *cac*) dispersed in (A) aqueous HCl (0.06 M); and (B) aqueous NaBF₄ (0.025 M) at 60 $^{\circ}\text{C}$ as a function of time. Spectra were measured after the pH stabilization in case of aqueous NaBF₄. Due to solubility limitation, low concentration of amphiphile **1** was used. However, it is above *cac* ($\approx 5 \mu\text{M}$) in the aqueous medium (Ref. 1)

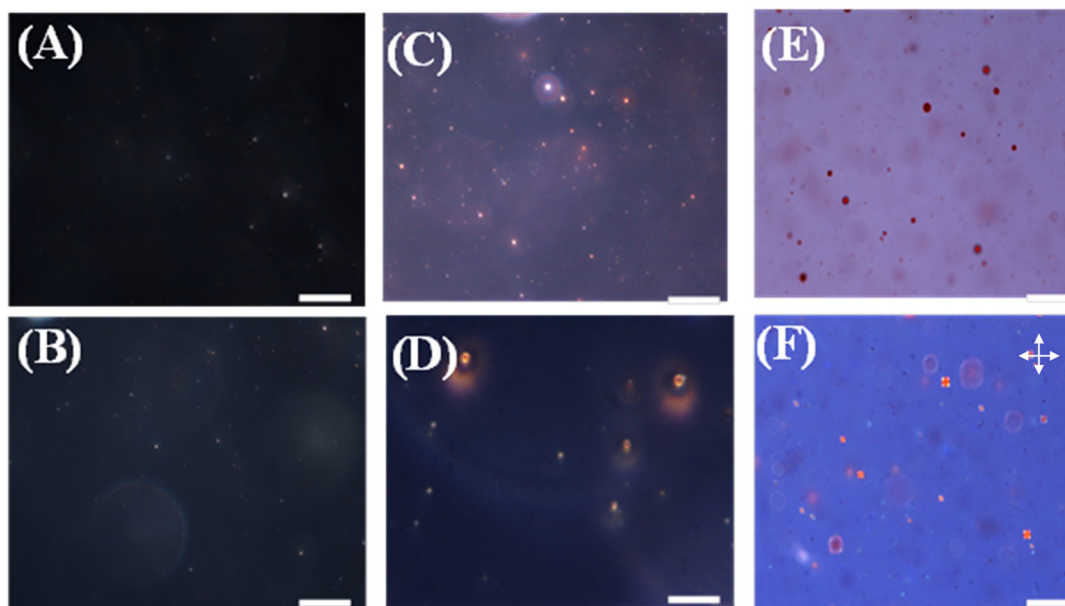


Fig. S14. Darkfield optical microscopic images of amphiphile **1** (500 μM) dispersed in $[\text{C}_2\text{mim}][\text{C}_2\text{OSO}_3]$ -water mixtures (IL; 10 vol %) at 25 $^\circ\text{C}$ under varying conditions: (A) as prepared (without HCl); (B) after 1 heating-cooling cycle (without HCl); (C) just prepared dispersions under acidic conditions (HCl = 0.02 M); (D) after repeating 5 heating-cooling cycles for dispersions shown in (C). Here, the effect of added Cl^- ion concentration is considered to be negligible compared to the high concentration of IL (ca. 0.56 M) employed (IL content of 10 vol%). (E) and (F) are the bright field and DFOM images of dispersions shown in (D). Scale bar is 5 μm .

Table S1. pH of various water–ILs systems (ILs: 10 vol%) at room temperature regarded as “as-prepared” samples and after one heating-cooling cycle (95 °C for 15 min).

ILs	as prepared	after heating-cooling
[C ₂ mim][BF ₄]	pH 3.6	pH 1.7
[C ₂ Py][BF ₄]	pH 4.3	pH 1.9
[C ₁ C ₃ Pip][BF ₄]	pH 4.2	pH 1.9
[C ₁ C ₂ Pyrr][BF ₄]	pH 4.0	pH 1.7